HHS Public Access

Author manuscript

AAPS J. Author manuscript; available in PMC 2019 February 08.

Published in final edited form as:

AAPS J. 2017 May ; 19(3): 703–711. doi:10.1208/s12248-017-0045-0.

Colloidal Gels with Extracellular Matrix Particles and Growth Factors for Bone Regeneration in Critical Size Rat Calvarial Defects

Jakob M. Townsend[1], **S. Connor Dennis**[2], **Jonathan Whitlow**[2], **Yi Feng**[3], **Jinxi Wang**[3], **Brian Andrews**[4], **Randolph J. Nudo**[5], **Michael S. Detamore**[1], and **Cory J. Berkland**[2,6,7]

[1]Stephenson School of Biomedical Engineering, University of Oklahoma, Norman, Oklahoma 73019, USA. [2]Bioengineering Program, University of Kansas, Lawrence, Kansas 66047, USA. [3]Department of Orthopedic Surgery, University of Kansas Medical Center, Kansas City, Kansas 66160, USA. [4]Department of Plastic Surgery, University of Kansas Medical Center, Kansas City, Kansas 66160, USA. [5]Department of Rehabilitation Medicine, University of Kansas Medical Center, Kansas City, Kansas 66160, USA. [6]Department of Pharmaceutical Chemistry, University of Kansas, Lawrence, Kansas 66047, USA. [7]To whom correspondence should be addressed. (berkland@ku.edu)

Abstract

Colloidal gels encapsulating natural materials and exhibiting paste-like properties for placement are promising for filling complex geometries in craniofacial bone regeneration applications. Colloidal materials have demonstrated modest clinical outcomes as bone substitutes in orthopedic applications, but limited success in craniofacial applications. As such, development of a novel colloidal gel will fill a void in commercially available products for use in craniofacial reconstruction. One likely application for this technology is cranial reconstruction. Currently, traumatic brain injury (TBI) is often treated with a hemicraniectomy, a procedure in which half the cranium is removed to allow the injured brain to swell and herniate beyond the enclosed cranial vault. The use of colloidal gels would allow for the design of a pliable material capable of expansion during brain swelling and facilitate cranial bone regeneration alleviating the need for a second surgery to replace the previously removed hemi-cranium. In the current study, colloidal nanoparticles of hydroxyapatite (HAp), demineralized bone matrix (DBM), and decellularized cartilage (DCC) were combined with hyaluronic acid (HA) to form colloidal gels with desirable rheological properties ($\tau_y \geq 100$ Pa). BMP-2 and VEGF growth factors were included to assess extracellular matrix (ECM) contribution of DBM and DCC. The HA-HAp (BMP-2) and HA-HAp-DCC group had 89 and 82% higher bone regeneration compared to the sham group, respectively ($p < 0.01$). Material retention issues observed may be alleviated by implementing chemical crosslinking. Overall, DCC may be a promising material for bone regeneration in general, and colloidal gels may hold significant potential in craniofacial applications.

Keywords

colloidal gel; decellularized cartilage; extracellular matrix; hyaluronic acid; hydroxyapatite

INTRODUCTION

Colloidal gels represent a promising class of injectable materials for use in tissue engineering and regenerative medicine applications because of their high water content, self-assembly, tunable mechanical properties, and implementation of physical crosslinking for minimally invasive delivery (1). The use of physical crosslinking principles in the development of colloidal hydrogels has resulted in the creation of highly tunable rheological properties capable of exhibiting yield stress for surgical placement and material recovery after injection (2–4). In our previous studies utilizing colloidal gel technologies, these properties have been mapped using polymers and colloidal particles to achieve “paste-like” properties ideal for surgical placement (1,5). One clinical specialty that will greatly benefit from colloidal gel technology used for bone regeneration is craniofacial surgery (6). Previous studies have demonstrated that similar colloidal gels have shown promise in bone tissue engineering applications, highlighting the use of biodegradable natural materials as an attractive alternative to current commercially available options (7,8).

Current commercial products have demonstrated a long track record of clinical success in orthopedic long bone regeneration; however, many craniofacial applications are limited by current product designs and physical properties (9). In particular, cranial reconstruction has been problematic due to the large contoured surface area, the constant repetitive pulsation of the underlying dura/brain, limited soft tissue coverage options, and sensitivity of the underlying brain tissue to exothermic biomaterial processes. Commercially available products such as DBX (MTF/Synthes), Dynagraft II (Integra Orthobiologics), Grafton® Gel (Osteotech), and Puros® DBM (Zimmer) have had limited success in calvarial reconstruction due to the low availability of propriogenic stem cells in the cranial diploic space as compared to that of long bones and the inability of all biomaterials to overcome a critical cranial defect size. These limitations of current commercial bone products have led to the need for new materials, and as such, new and innovative approaches should be considered for future cranial bone regenerative biomaterials.

Current bone products focus heavily on the use of micron-sized demineralized bone matrix (DBM) colloids as a tissue matrix/scaffold for the promotion of cranial bone formation. Since these materials require bone ingrowth from the surrounding peripheral cranial margins, critical cranial defect size limits the ability to reconstruct large skull defects. To address the limited bone regeneration associated with demineralized bone techniques, various synthetic and raw materials, such as extracellular matrix (ECM) components, have been proposed for tissue regeneration such as hydroxyapatite (HAp), Bioglass, hyaluronic acid (HA), DBM, and decellularized cartilage (DCC) (10,11). Growth factors such as bone morphogenetic protein (BMP)-2 and vascular endothelial growth factor (VEGF) have shown further promise in bone regeneration, and can be used both separately or by dual delivery (12,13). The majority of craniofacial skeleton forms by intramembranous (IM) ossification; however, leveraging endochondral (EC) ossification approaches for regeneration of craniofacial bone may provide novel medical treatment avenues (14).

A clinical application that could greatly benefit from a medical product exhibiting paste-like rheological properties and bone regenerative potential is the surgical management of severe

traumatic brain injury (TBI). TBI resulting from a severe closed head injury or stroke often causes life-threatening brain swelling (15). Decompressive hemicraniectomy is a life-saving treatment to alleviate brain swelling. In this procedure, approximately half of the patient's calvarial bone is removed allowing the brain to swell and herniate beyond the confines of the closed calvarial vault (16). This skin is draped over the herniating brain and the skull is left removed for an average of 80 days before it is restored/replaced once swelling subsides in a second surgical procedure, cranioplasty (17). This surgical procedure gained popularity with its utilization and proven beneficial outcomes in the treatment of active duty service who suffer severe head trauma in recent military conflicts. These soldiers represent a group that has been greatly impacted by TBI, referred to as the "invisible war on the brain" (18) and accounting for 30% of military hospitalizations during modern warfare (19).

A poorly understood neurologic condition termed "syndrome of the trephined" (SoT) often results in TBI patients who undergo hemi-craniectomy. SoT is also termed "sinking skin flap syndrome" as a result of the sunken, concave appearance of the skull at the sight of hemi-craniectomy that develops as TBI patients await cranioplasty (20,21). SoT is associated with symptoms such as mood changes, fatigue, headaches, dizziness, fine motor dexterity problems, and difficulties concentrating (22). Interestingly, SoT neurologic deficits are immediately reversible with a cranioplasty procedure where the missing cranial bone is replaced/restored and the underlying sunken cerebral tissue is allowed to re-expand within the calvarial vault. The symptoms typically return should the cranioplasty reconstruction require future removal such as the case of infection.

Current surgical management of TBI requires a two-staged procedure: the initial hemi-craniectomy and the reconstructive cranioplasty. They are typically performed months apart which delay recovery and rehabilitation and increasing cost and risk due to an additional surgery (23,24). Research on materials for TBI treatment has generally focused on reducing brain swelling (25,26) or blocking tissue regeneration between the dura and periosteum for safer transition to cranioplasty (17). Colloidal gel technology has the potential to provide a single-surgical treatment for severe TBI cases in which the material is implanted with the initial surgery, remain pliable during brain swelling, and provide a combination of materials and growth factors to regenerate bone over time.

To effectively develop a material capable of providing a single surgery for TBI treatment, we must first identify an effective colloidal gel formulation that can regenerate bone across a critical size calvarial defect. After identifying a colloidal gel that can regenerate bone in a critical size defect, the regeneration time can be tuned specifically for treatment of TBI. The objective of this work was to evaluate colloidal gels composed of natural materials and growth factors for regenerating calvarial bone in a critical size calvarial defect. The use of natural materials is our first attempt with this type of formulation and represents a next generation colloidal gel from our previously published work by Wang *et al.* (6) HAp, DBM, or DCC nanoparticles were evaluated in physically crosslinked colloidal gel formulations with HA to create paste-like materials with desirable yield stress for injection in a bone regeneration application. Colloidal gel material characterization studies have previously been published by Dennis *et al.* (27), colloidal formulations with desirable mechanical properties were chosen for evaluation in the current study. Colloidal gels were loaded with

or without BMP-2 and VEGF to evaluate the extent to which growth factors would facilitate bone regeneration. We hypothesized that the colloidal gel formulations would regenerate bone at the defect site, and that the addition of DCC particles would increase regenerative capabilities.

MATERIALS AND METHODS

Materials

Hydroxyapatite (HAp) was purchased in powder form ($D_{avg} \leq 200$ nm; Sigma-Aldrich, St. Louis, MO). Hyaluronic acid (HA, Mw = 1.01–1.8 MDa) (Lifecore Biomedical, Chaska, MN) was purchased as a sodium salt. Human DBM was purchased from Biomet (Warsaw, IN). Human VEGF (Cat# 100–20) and human BMP-2 (Cat# 120–02) were purchased from PeproTech (Rocky Hill, NJ).

Preparation of Decellularized Cartilage (DCC)

Ten porcine knees were purchased from a local abattoir (Bichelmeyer Meats, Kansas City, KS). Articulating hyaline cartilage was harvested from mixed-breed, mixed-sex hogs 7–8 months of age. Harvested cartilage was coarse ground using a cryogenic tissue grinder (BioSpec Products, Bartlesville, OK) and packed into dialysis tubing (3500 MWCO) and decellularized using an adapted version of our previously established method using osmotic shock, detergent, and enzymatic washes (28–30). Briefly, dialysis packets containing DCC were placed in a hypertonic salt solution (HSS) overnight at room temperature under agitation (70 rpm). The packets were then subjected to 220 rpm agitation and washed in Triton X-100 (0.01 *v*/*v*) followed by HSS, with DI washes between each step, to permeabilize intact cellular membranes. Tissue packets were then treated with benzonase enzyme solution (0.0625 KU/mL) at 37°C overnight followed by DI washing, and then treated with sodium-lauroylsarcosine (NLS, 1% *v*/*v*) overnight to lyse cells and denature proteins. After NLS treatment, the tissue was washed in DI water, and then in 40% (*v*/*v*) ethanol at 70 rpm. Tissue packets were then subjected to organic exchange resins and to remove organic material from solution. Tissue packets were then washed in a saline-mannitol solution at 70 rpm followed by 1 h of DI washes. The tissue was then removed from the dialysis packets and frozen.

After the decellularization process, DCC particles were lyophilized and cryoground with a freezer-mill (SPEX, SamplePrep, Metuchen, NJ). Cryoground DCC was then sieved (Spectra/Mesh Woven Filters, Spectrum Laboratories, Inc., Rancho Dominguez, CA) ($D_{avg} \leq 200$ nm) and stored at −20°C for later use. Decellularization was confirmed by PicoGreen (Thermo Fisher Scientific, Waltham, MA, P7589) assay to determine DNA content. The particle size ranges of DCC and HAp were confirmed using dynamic light scattering (Brookhaven, ZetaPALS) as previously described (5).

Preparation of Colloidal Gels

Colloidal gels were prepared as previously described (5). Briefly, 20 mg of HA, 800 mg of HAp, and 150 mg of ECM (DCC or DBM) materials were weighed dry and combined. Dry combinations were dispersed in 1 mL of phosphate-buffered saline (PBS, Sigma-Aldrich,

P3813) solution. Dry powder formulations were sterilized using ethylene oxide gas prior to use *in vivo*. PBS and growth factors were mixed together (25 μg/mL) in select groups before dispersion of dry powder combinations. Samples were allowed to reach ambient conditions for 2 h before implanting. Formulations are reported as material components with the addition of growth factors in parentheses [e.g., HA-HAp (VEGF)].

Environmental Scanning Electron Microscopy (ESEM)

Colloidal gels were imaged using an FEI Quanta 200 scanning electron microscope (FEI Company, Hillsboro, OR) with a tungsten filament electron source. The gaseous secondary electron detector (GSED) was used in environmental mode. Samples were imaged at a magnification of approximately 500×, and an accelerating voltage of 15 kV.

Rheological Testing

Colloidal gel rheological properties were mapped using a controlled stress rheometer (TA-Instruments, AR2000). All measurements were performed at a gap distance of 500 μm using a 20-mm diameter roughened stainless steel plate geometry. Samples were tested at 37°C. Initially, an oscillatory stress sweep from 1 and 10,000 Pa was performed at a constant frequency of 1 Hz to determine the linear viscoelastic (LVE) region for the colloidal formulations. The yield stress was defined as the oscillatory stress corresponding to a 15% departure of the storage modulus (G') from the LVE region.

Animal Model and Surgical Method

Mixed-sex SAS Sprague Dawley rats were raised in house to an age of 7–10 weeks and randomly assigned to treatment groups prior to surgery. Animal experiments were approved by the Institutional Animal Care and Use Committee of the University of Kansas Medical Center (protocol #2015–2303). A posterior incision along the periphery of the skull was created to peel back and suture the skin and periosteum to the anterior portion of the skull. A single critical size 7.5 mm defect was created on the center of the calvarial bone using a cylindrical drill. The calvarial disk was carefully removed leaving the dura matter intact. After creation of the defect, approximately 50 μL of material was used to fill the site via syringe (Fig. 1a). The skin and periosteum were then draped over the defect site and sutured in place to hold the material during the healing process. The sham group received the same surgical procedure without the addition of any further treatment. Repaired tissue was harvested at 8 weeks' post-implantation and analyzed. A sample size of five rats was used in BMP-2 containing groups, and a sample size of four rats was used in all other groups.

Micro-computed Tomography (μCT)

Micro-computed tomography analysis was performed on explanted rat calvarial sections to visualize and quantify new bone formation. An Xradia MicroXCT-400 system was used with a 50-kV X-ray source at 7.9 W. μCT images were reconstructed to generate 3D models for analysis of new bone formation. Avizo-Fire computational software (FEI Company) was used to generate 3D images and quantify volumes. New bone was confirmed using pre-existing calvarial bone as the threshold, separating original HAp from new bone formed. HAp nanoparticles were partitioned from bone on the basis that any material above the bone

threshold must be original HAp. Quantified new bone volume is expressed as a total (mm^3) within the 7.5-mm diameter defect site.

Histology and Immunohistochemistry

Harvested calvarial bone samples were fixed in 10% phosphate-buffered formalin for 48 h then stored in 70% ethanol for long term. Tissue sections were then decalcified using Calrite media (Thermo Fisher Scientific, 22-046-339) for 3 weeks before dehydrating in a grade series of ethanol to xylenes, and then embedded in paraffin wax. Sections of 5 μm were obtained using a microtome (Thermo Fisher Scientific, HM 355S) and affixed to microscope slides. Before staining, tissue sections were dewaxed in xylene and rehydrated in graded (i.e., 100 to 70%) ethanol followed by deionized water. Slides were stained with hematoxylin and eosin (H&E) (Abcam, Cambridge, UK, H-3404) for cell infiltration and new bone formation.

Immunohistochemistry was employed to visualize the distribution of collagen I (Novus Biological, Littleton, CO, NB600–408, 10 μg/mL), collagen II (Novus Biological, NBP2–33343, 5 μg/mL), osteocalcin (Abcam, ab93876, 5 μg/mL), and α-smooth muscle actin (Abcam, ab5694, 10 μg/mL). Briefly, tissue sections were dewaxed in xylenes and rehydrated in a graded series of ethanol (100–70%) to DI water. Antigen retrieval was performed enzymatically with proteinase K (Abcam, ab64220, 20 μg/mL) for 15 min at 37°C. Following enzymatic retrieval, sections were blocked with 0.3% hydrogen peroxide (Abcam, ab94666) for 10 min, 10% normal horse serum (Vector Labs, Burlingame, CA, PK-6200) for 20 min, 5% bovine serum albumin (Sigma, A9647) for 20 min, and avidin/biotin blocking (Vector Labs, SP-2001) for 15 min each. Sections were incubated in one of the aforementioned primary antibodies for 1 h. Post-primary antibody incubation, sections were washed in PBS with Tween-20 (Sigma-Aldrich, P3563) solution for 5 min between each step. Sections were then incubated with biotinylated horse anti-mouse/rabbit IgG (Vector Labs, PK-6200) for 30 min. Sections were then incubated with VECTASTAIN Elite ABC solution (Vector Labs, PK-6200) for 30 min, before being developed using DAB (Vector Labs, SK-4100) for 2 min. DAB-enhancing solution (Vector Labs, H-2200) was used for 10 s before counter-staining with hematoxylin QS (Vector Labs, H-3404) for 1 min. Bluing solution (Thermo Fisher Scientific, 7301) was used for 3 min. Finally, sections were dehydrated in a grade series of ethanol (95–100%) to xylenes before mounting. Negative controls for each immunohistochemical staining batch were included.

Statistical Methods

GraphPad Prism (Graphpad Software Inc, La Jolla, CA) statistical software was used to conduct all statistical analyses. Groups were analyzed using a one-way analysis of variance with groups of factors. Dunnett's test was used to compare groups to the sham control group. Tukey's HSD test was used for comparing between groups in the rheological analysis. Results were considered significant at a level of $p < 0.05$. Results are reported as the mean ± standard deviation.

RESULTS

Rheological Analysis

Figure 1b shows colloidal material groups being shaped, and ESEM images of the gel microstructure. Colloidal material shaping demonstrated that all formulations exhibited some degree of yield stress. Representative rheometer traces for each colloidal formulation have been provided (Fig. 2a–c). The yield stress of the HA-HAp-DBM was 4.6 times higher than the HA-HAp formulation ($p < 0.01$) (Fig. 2d). Post-hoc analysis (Tukey's HSD) showed no statistically significant difference between HA-HAp and HA-HAp-DCC, or between HA-HAp-DBM and HA-HAp-DCC formulations.

Micro-computed Tomography (μCT) Analysis

The HA-HAp (BMP-2) and HA-HAp-DCC groups had 89 and 82% higher regenerated bone volume compared to the sham, respectively (Fig. 3a, $p < 0.01$). Peripheral bone growth was noted in all groups, and large peripheral bone growth into the defect site in the HA-HAp-DCC group without the addition of growth factors (Fig. 3b). Large bone island formation was noted in the sham and VEGF-containing groups, excluding the group containing DCC. Bone islands observed in all groups were very thin compared to the native bone, and did not contribute significantly to regenerated bone volume.

Histological Analysis

A distinctive soft tissue formation spanning the defect site was observed in all colloidal gel formulations (Fig. 4). The presence of conglomerated colloidal particles was observed in all groups. Bone at the defect periphery was noted in all groups with new bone forming toward the dural side of the defect. The H&E stain confirmed the differences in new bone formation *versus* original colloidal particles identified from the μCT analysis. Histological analysis of all samples showed general trends of bone formation encapsulating conglomerated colloidal particles in HA-HAp groups with and without addition of growth factors. VEGF-containing groups tended to have thicker soft tissue formation spanning the defect site compared to groups without the addition of growth factors and the sham. The HA-HAp-DCC group and the BMP-2 groups had more peripheral bone growth into the defect site compared to the sham and VEGF-containing groups.

Immunohistochemical (IHC) Analysis

Visual results of all samples stained for COL1 show substantial deposition of COL1 in the tissue spanning the defect site using peripheral bone for reference (Fig. 5). COL2 deposition in all groups was near non-existent in the tissue spanning the defect site, except for DCC groups with addition of growth factors, with the DCC (BMP-2) group in particular showing more regions of collagen II than the DCC (VEGF) group. COL2 deposition in groups containing DCC and growth factors resulted in positive staining tissue pockets within the defect site; however, this was not seen in DCC samples without growth factors. OCN staining was similar to COL1 staining in that all groups showed positive antibody staining throughout the defect site using the peripheral bone as a reference. αSMA staining was

positive only in the soft tissue spanning the defect site and no staining in the bone portion as expected.

DISCUSSION

The current study was the first to use naturally derived decellularized cartilage extracellular matrix for regeneration of calvarial bone (14). Colloidal gels formulated of naturally derived ECM materials were evaluated with and without growth factors to determine osteogenic potential *in vivo*. The focus of this work in developing colloidal gels with physical crosslinking properties for ease of placement and pliability during the healing process is ideally positioned for the treatment of TBI after hemi-craniectomy (1,5). The proposed work is one of the few to propose a material capable of providing a single-surgical method for severe TBI treatment, eliminating the need for a second surgery to reclose the cranial vault (31). A single-surgical intervention for TBI has great implications for increasing the quality of life for the people suffering from this issue, and decreased time for rehabilitation. In developing these colloidal materials, our team has proposed the use of nanoparticle-size DBM and DCC as natural materials for the promotion of new bone growth.

Colloidal gels exhibiting a yield stress sufficient to create a paste-like consistency may have great clinical relevance for material placement and retention. Colloidal gels rely on physical interactions and the presence of a suitable yield stress in lieu of covalent crosslinking for material retention. The formulations presented in the current study were all capable of forming a paste-like material, and the addition of ECM materials further increased the yield stress observed. ESEM images of the gel microstructure indicated that the addition of ECM particles reduced cavitation, contributing to the mechanical stability. An increased yield stress in colloidal gels has implications for the improvement of mechanical performance in surgical placement and retention in the defect site (1). Although rheological testing confirmed the existence of a noticeable yield stress in all formulations, challenges with material retention were observed in the current study. In all cases, the majority of migrated material had moved anteriorly, possibly due to the normal head grooming motion of rats. Alternatively, the migration of HAp particles can possibly be attributed to material disintegration due to the lack of gel crosslinking after placement. The post-μCT analysis allowed for the ability to better assess regenerative capabilities by quantifying the volume of bone excluding the colloidal material, while subsequently visualizing the two. Other groups have previously used similar techniques for eliminating the quantification of non-bone material (32); however, it is not uncommon to report regenerated new bone volume including the added material (33). The result of the DCC material group without growth factors supports the idea that cartilage can be used as a raw material for use in a paste-like application for calvarial bone regeneration.

Aggregation of HAp particles was noted in all samples analyzed, suggesting interaction between HAp nanoparticles to form larger clusters. Bone growth around the HAp clusters was visualized by H&E stain, supporting the osteoconductive properties of HAp. Possible osteoinductive potential was observed in the form of new bone islands throughout the defect site without the presence of HAp particles; however, bone island formation was also noted in the sham group. In all samples, a noticeable tissue had formed throughout the defect site.

Small pockets of positive COL2 staining were noted in the DCC group containing BMP-2, leading to the suggestion that growth factor addition had a negative role on cell differentiation in the presence of the material DCC. The result may potentially be attributed to competing effects of DCC and BMP-2, or a synergistic effect of chondrogenesis rather than osteogenesis leading to delayed bone regeneration. COL2 deposition was not observed in the group containing DCC without growth factors, suggesting that including DCC may have provided osteoinductive potential. Consistent positive staining in all groups for COL1 and OCN can most likely be attributed to the common material HA-HAp in all groups. Additionally, results of αSMA staining showed a positive response in the soft tissue portion of the defect site; however, increased blood vessel formation was not observed in VEGF-treated groups. Addition of BMP-2 did not produce the bone regeneration that had been previously observed in similar studies in rat calvarial defects. Cowan *et al.* (34) observed a significant increase in bone formation with the addition of 30 μg/mL of BMP-2 (0.59 μg total); however, this was not observed in the current study using 25 μg/mL of BMP-2 (1.25 μg total). The differences observed emphasize the value of future growth factor dose response studies. The low amount of new bone regeneration in growth factor-containing groups could possibly be due to a fast release from the defect site, causing a low response to available stem cells. Future studies including growth factors will include a controlled release mechanism for optimal delivery, and characterizing growth factor release *in vitro*, as the release profile would have been of great value in the current study.

The addition of natural materials, i.e., DBM or DCC, had unexpected results in terms of bone regeneration potential. On average, the addition of DBM did not increase the regenerative potential compared to HA-HAp hydrogels, whereas addition of DCC had produced greater bone regeneration on average compared to DBM groups. DCC samples without growth factors were observed to have large amounts of peripheral bone growth, suggesting potential for DCC in calvarial bone regenerative approaches. Regenerated bone volumes of all groups tested in the current study were within the range of previously published studies in the area, and on average the HA-HAp (BMP-2) and HA-HAp-DCC group had more regenerated bone volume (32,35). Other groups studying the use of cartilage ECM for bone regeneration observed similar findings compared to the current study. In a study by Visser *et al.* (36) using decellularized cartilage ECM particles embedded in gelatin methacrylamide hydrogels found mineralized bone surrounding hypertrophic cartilage. Similarly, Gawlitta *et al.* (37) found that bone formation was greatly enhanced by the presence of mesenchymal stem cells in decellularized cartilage ECM scaffolds. The collective results from the studies previously mentioned and the current study further support the use of DCC in bone regeneration applications. Caution should be taken in comparing the results of the current study due to the randomized sex study design. The National Institute of Health (NIH) notice (NOT-OD-102) “Consideration of Sex as a Biological Variable in NIH-funded Research” has identified an over-reliance on male animals and cells in research. The random use of both sexes in the current study attempts to follow NIH guidelines to eliminate sex as a variable.

Poor retention of growth factors and colloidal materials in the defect site was observed in the current study. Retention issues may be fixed by implementing a covalent crosslinking mechanism after material placement. A tunable crosslinking mechanism would effectively

provide material stiffness and allow for recovery after non-plastic deformation. The crosslinking can be tuned accordingly to create hydrogels that remain pliable enough for application in the treatment of TBI. In future studies, colloidal materials encapsulated in covalently crosslinked hydrogels will be explored for application to craniofacial bone regeneration.

CONCLUSION

Colloidal gels composed of polymers and tissue particles represent a promising material for bone regenerative approaches, specifically in their ability to exhibit paste-like properties for surgical placement. The study evaluated bone regeneration of critical size (7.5 mm) rat calvarial defects using colloidal gels comprised of hyaluronic acid, hydroxyapatite, and tissue particles (DCC or DBM) with and without the addition of growth factors (BMP-2 and/or VEGF). All colloidal formulations exhibited suitable yield stress for material placement and an increased yield stress performance with the addition of DBM or DCC particles. Significant bone volume regeneration was observed in the HA-HAp (BMP-2) and HA-HAp-DCC group compared to the sham defect after 8 weeks. The results suggest that the material DCC has osteogenic potential for bone regeneration applications. Colloidal gels incorporating natural ECM materials have promise for calvarial bone regeneration applications.

ACKNOWLEDGEMENTS

The authors would like to thank Dr. Emily Beck for her assistance with the cartilage decellularization process. We would like to recognize funding from the National Institutes of Health (R01 DE022472) and from the Kansas Bioscience Authority Rising Star Award.

REFERENCES

1. Beck EC, Lohman BL, Tabakh DB, Kieweg SL, Gehrke SH, Berkland CJ, et al. Enabling surgical placement of hydrogels through achieving paste-like rheological behavior in hydrogel precursor solutions. Ann Biomed Eng. 2015;43(10):2569–76. [PubMed: 25691398]
2. Fakhari A, Phan Q, Berkland C. Hyaluronic acid colloidal gels as self-assembling elastic biomaterials. J Biomed Mater Res B Appl Biomater. 2014;102(3):612–8. [PubMed: 24124008]
3. Guvendiren M, Lu HD, Burdick JA. Shear-thinning hydrogels for biomedical applications. Soft Matter. 2012;8(2):260–72.
4. Lu HD, Charati MB, Kim IL, Burdick JA. Injectable shear-thinning hydrogels engineered with a self-assembling Dock-and-Lock mechanism. Biomaterials. 2012;33(7):2145–53. [PubMed: 22177842]
5. Dennis SC, Detamore MS, Kieweg SL, Berkland CJ. Mapping glycosaminoglycan-hydroxyapatite colloidal gels as potential tissue defect fillers. Langmuir. 2014;30(12):3528–37. [PubMed: 24606047]
6. Wang Q, Gu Z, Jamal S, Detamore MS, Berkland C. Hybrid hydroxyapatite nanoparticle colloidal gels are injectable fillers for bone tissue engineering. Tissue Eng A. 2013;19(23–24):2586–93.
7. Wang Q, Jamal S, Detamore MS, Berkland C. PLGA-chitosan/PLGA-alginate nanoparticle blends as biodegradable colloidal gels for seeding human umbilical cord mesenchymal stem cells. J Biomed Mater Res A. 2011;96(3):520–7. [PubMed: 21254383]
8. Wang Q, Wang L, Detamore MS, Berkland C. Biodegradable colloidal gels as moldable tissue engineering scaffolds. Adv Mater. 2008;20(2):236–9.
9. Gruskin E, Doll BA, Futrell FW, Schmitz JP, Hollinger JO. Demineralized bone matrix in bone repair: history and use. Adv Drug Deliv Rev. 2012;64(12):1063–77. [PubMed: 22728914]

10. Renth AN, Detamore MS. Leveraging “raw materials” as building blocks and bioactive signals in regenerative medicine. Tissue Eng B Rev. 2012;18(5):341–62.
11. Wu Z, Fan L, Xu B, Lin Y, Zhang P, Wei X. Use of decellularized scaffolds combined with hyaluronic acid and basic fibroblast growth factor for skin tissue engineering. Tissue Eng A. 2015;21(1–2):390–402.
12. Patel ZS, Young S, Tabata Y, Jansen JA, Wong ME, Mikos AG. Dual delivery of an angiogenic and an osteogenic growth factor for bone regeneration in a critical size defect model. Bone. 2008;43(5):931–40. [PubMed: 18675385]
13. Young S, Patel ZS, Kretlow JD, Murphy MB, Mountziaris PM, Baggett LS, et al. Dose effect of dual delivery of vascular endothelial growth factor and bone morphogenetic protein-2 on bone regeneration in a rat critical-size defect model. Tissue Eng A. 2009;15(9):2347–62.
14. Dennis SC, Berkland CJ, Bonewald LF, Detamore MS. Endochondral ossification for enhancing bone regeneration: converging native extracellular matrix biomaterials and developmental engineering in vivo. Tissue Eng B Rev. 2015;21(3):247–66.
15. Omary R, Chernoguz D, Lasri V, Leker RR. Decompressive hemicraniectomy reduces mortality in an animal model of intracerebral hemorrhage. J Mol Neurosci. 2013;49(1):157–61. [PubMed: 23152135]
16. Marquez-Rivas J, Rivero-Garvia M, Mayorga-Buiza MJ, Rodriguez - Boto G. Craniectomy. J Neurosurg. 2013;119(6):1657.
17. Oladunjoye AO, Schrot RJ, Zwienenberg-Lee M, Muizelaar JP, Shahlaie K. Decompressive craniectomy using gelatin film and future bone flap replacement. J Neurosurg. 2013;118(4):776–82. [PubMed: 23394343]
18. Alexander C The invisible war on the brain. Natl Geogr. 2015;1.
19. Risdall JE, Menon DK. Traumatic brain injury. Philos Trans R Soc Lond B Biol Sci. 2011;366(1562):241–50. [PubMed: 21149359]
20. Dujovny M, Agner C, Aviles A. Syndrome of the trephined: theory and facts. Crit Rev Neurosurg. 1999;9(5):271–8. [PubMed: 10525845]
21. Bijlenga P, Zumofen D, Yilmaz H, Creisson E, de Tribolet N. Orthostatic mesodiencephalic dysfunction after decompressive craniectomy. J Neurol Neurosurg Psychiatry. 2007;78(4):430–3. [PubMed: 17119005]
22. Schiffer J, Gur R, Nisim U, Pollak L. Symptomatic patients after craniectomy. Surg Neurol. 1997;47(3):231–7. [PubMed: 9068692]
23. Yang XF, Wen L, Shen F, Li G, Lou R, Liu WG, et al. Surgical complications secondary to decompressive craniectomy in patients with a head injury: a series of 108 consecutive cases. Acta Neurochir (Wien). 2008;150(12):1241–7. [PubMed: 19005615]
24. Stiver SI. Complications of decompressive craniectomy for traumatic brain injury. Neurosurg Focus. 2009;26(6):E7.
25. Tian WM, Hou SP, Ma J, Zhang CL, Xu QY, Lee IS, et al. Hyaluronic acid-poly-D-lysine-based three-dimensional hydrogel for traumatic brain injury. Tissue Eng. 2005;11(3–4):513–25. [PubMed: 15869430]
26. Wang Q, Wang J, Lu Q, Detamore MS, Berkland C. Injectable PLGA based colloidal gels for zero-order dexamethasone release in cranial defects. Biomaterials. 2010;31(18):4980–6. [PubMed: 20303585]
27. Dennis SC, Whitlow J, Detamore MS, Kieweg SL, Berkland C. Hyaluronic acid-hydroxyapatite colloidal gels combined with micronized native ECM as potential bone defect fillers. Langmuir. 2016.
28. Sutherland AJ, Beck EC, Dennis SC, Converse GL, Hopkins RA, Berkland CJ, et al. Decellularized cartilage may be a chondroinductive material for osteochondral tissue engineering. PLoS One. 2015;10(5):e0121966. [PubMed: 25965981]
29. Sutherland AJ, Detamore MS. Bioactive microsphere-based scaffolds containing decellularized cartilage. Macromol Biosci. 2015;15(7):979–89. [PubMed: 25821206]
30. Converse GL, Armstrong M, Quinn RW, Buse EE, Cromwell ML, Moriarty SJ, et al. Effects of cryopreservation, decellularization and novel extracellular matrix conditioning on the quasi-static

and time-dependent properties of the pulmonary valve leaflet. Acta Biomater. 2012;8(7):2722–9. [PubMed: 22484150]

31. Martin KD, Franz B, Kirsch M, Polanski W, von der Hagen M, Schackert G, et al. Autologous bone flap cranioplasty following decompressive craniectomy is combined with a high complication rate in pediatric traumatic brain injury patients. Acta Neurochir (Wien). 2014;156(4): 813–24. [PubMed: 24532225]
32. Vo TN, Shah SR, Lu S, Tatara AM, Lee EJ, Roh TT, et al. Injectable dual-gelling cell-laden composite hydrogels for bone tissue engineering. Biomaterials. 2016;83:1–11. [PubMed: 26773659]
33. Ferreira JR, Padilla R, Urkasemsin G, Yoon K, Goeckner K, Hu WS, et al. Titanium-enriched hydroxyapatite-gelatin scaffolds with osteogenically differentiated progenitor cell aggregates for calvaria bone regeneration. Tissue Eng A. 2013;19(15–16):1803–16.
34. Cowan CM, Aghaloo T, Chou YF, Walder B, Zhang X, Soo C, et al. MicroCT evaluation of three-dimensional mineralization in response to BMP-2 doses in vitro and in critical sized rat calvarial defects. Tissue Eng. 2007;13(3):501–12. [PubMed: 17319794]
35. Vo TN, Ekenseair AK, Spicer PP, Watson BM, Tzouanas SN, Roh TT, et al. In vitro and in vivo evaluation of self-mineralization and biocompatibility of injectable, dual-gelling hydrogels for bone tissue engineering. J Control Release. 2015;205:25–34. [PubMed: 25483428]
36. Visser J, Gawlitta D, Benders KEM, Toma SMH, Pouran B, van Weeren PR, et al. Endochondral bone formation in gelatin methacrylamide hydrogel with embedded cartilage-derived matrix particles. Biomaterials. 2015;37:174–82. [PubMed: 25453948]
37. Gawlitta D, Benders KE, Visser J, van der Sar AS, Kempen DH, Theyse LF, et al. Decellularized cartilage-derived matrix as substrate for endochondral bone regeneration. Tissue Eng A. 2015;21(3–4):694–703.

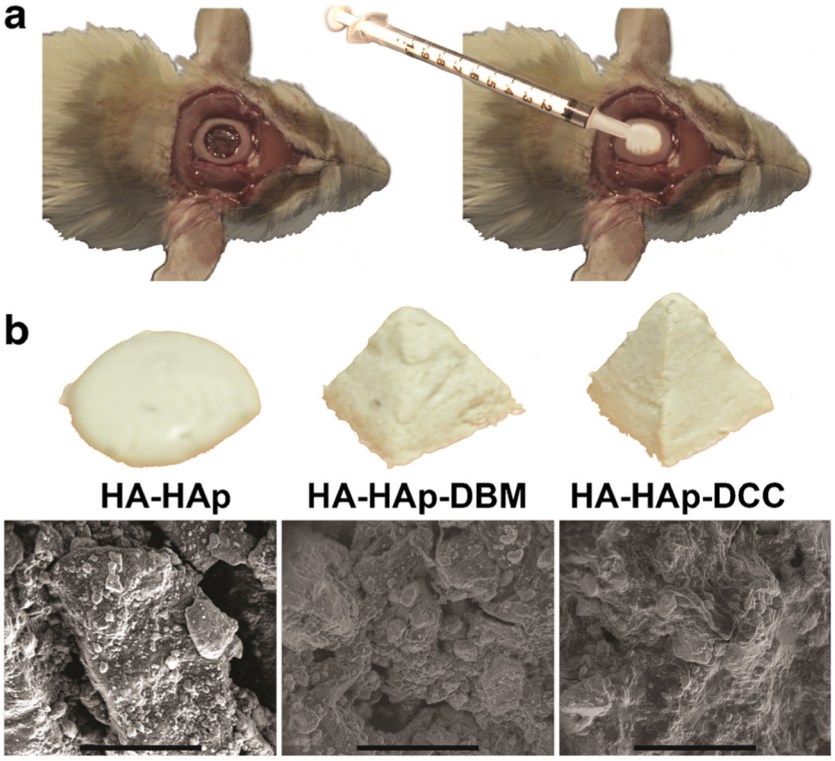

Fig. 1.

a Surgical method illustration shown in two steps, in the first (*left*) step the scalp is opened and a 7.5-mm cylindrical bone section is removed. The following step (*right*) involves filling the defect gap using a syringe loaded with one of the material groups and smoothing into place, before suturing the scalp back in place. **b** Extruded and shaped material groups of HA-HAp, HA-HAp-DBM, and HA-HAp-DCC. Material yield stress allowed for retention after shaping using a surgical spatula. Environmental scanning electron microscope images provide insight into the gel microstructure. Scale bars = 200 μm

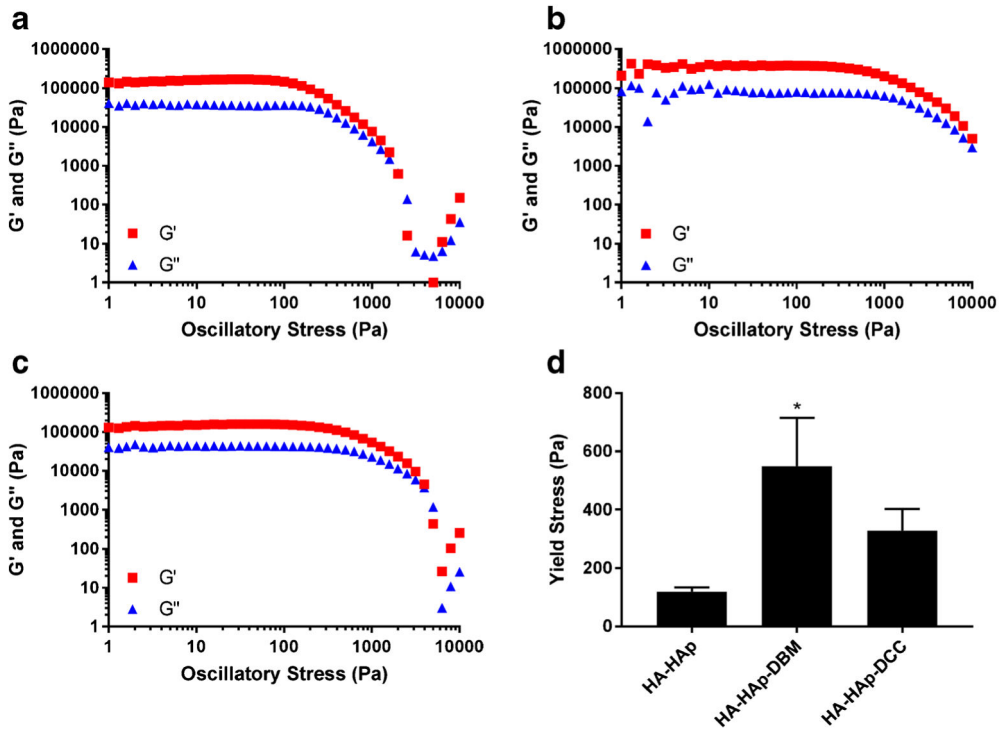

Fig. 2.

a–c Representative rheometer traces for HA-HAp, HA-HAp-DBM, and HA-HAp-DCC, respectively. **d** Colloidal gel yield stress corresponding to a 15% deviation of G' from linearity. Addition of DBM significantly increased the yield stress of the material compared to HA-HAp as indicated by an asterisk ($p < 0.01$)

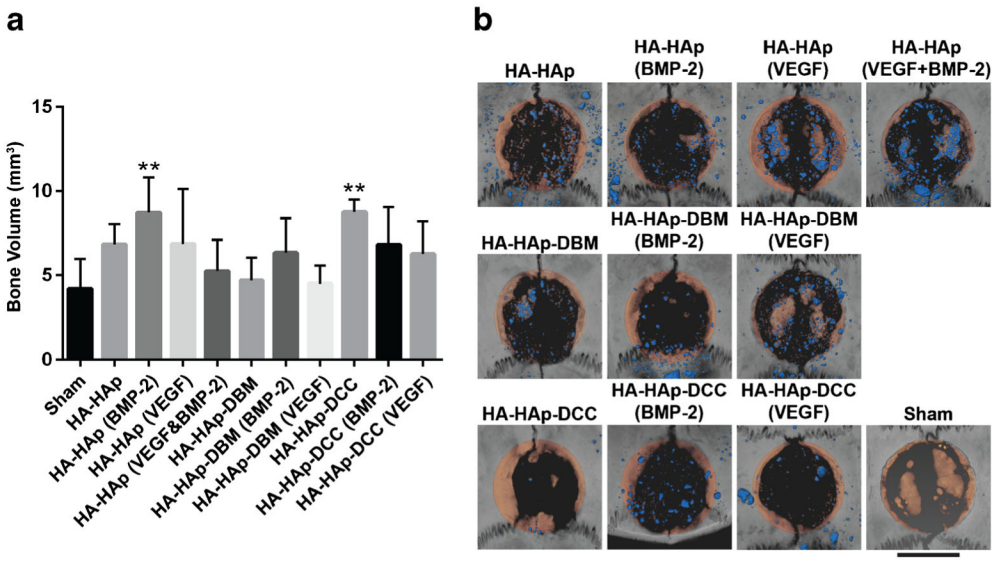

Fig. 3.

a *In vivo* regenerated bone volume. Bone regeneration was evaluated after 8 weeks using microcomputed tomography (μCT) analysis. *Asterisks* (**) represent statistically significant results ($p < 0.01$) compared to the sham. *Error bars* represent standard deviations. **b** μCT analysis using Avizo-Fire software. *Orange coloring* indicating the regenerated bone, and *blue coloring* defining original colloidal particles. *Scale bar* represents 5 mm in length

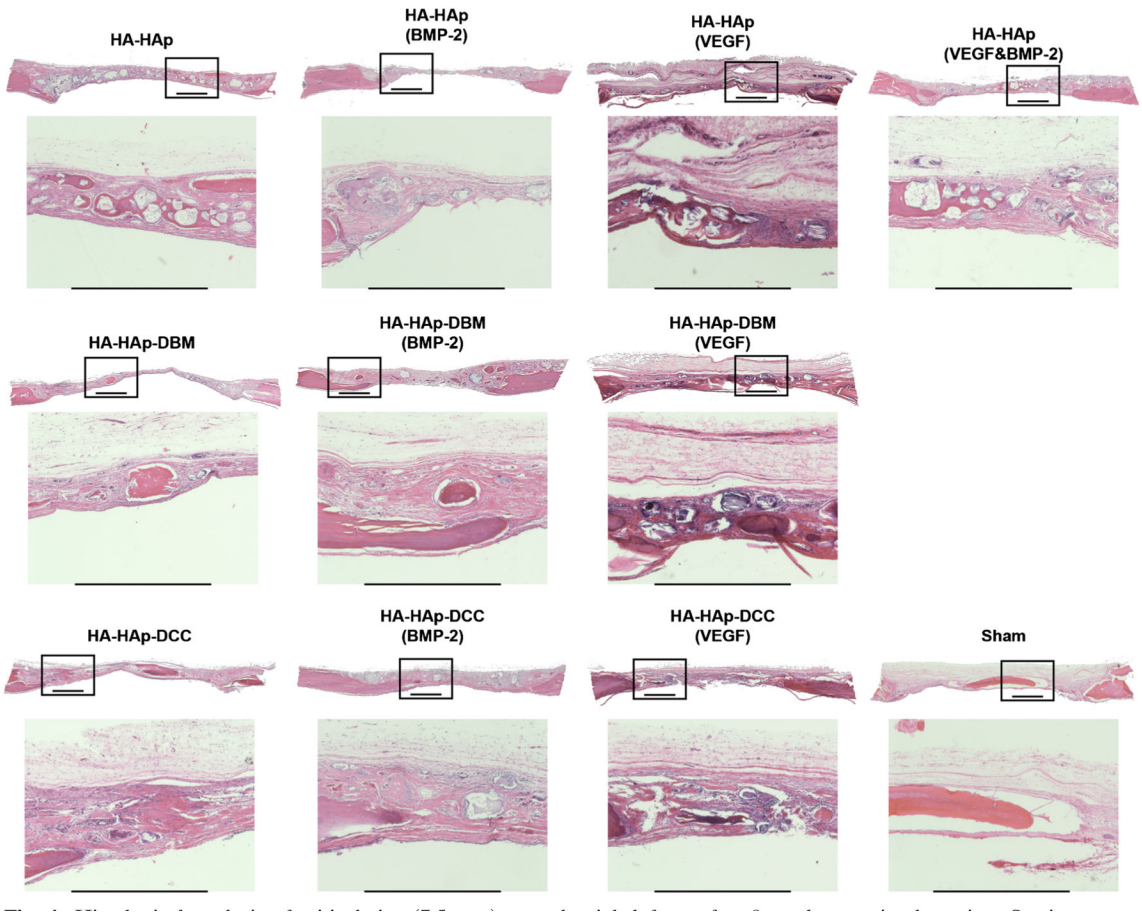

Fig. 4.

Histological analysis of critical size (7.5 mm) rat calvarial defects after 8 weeks post-implantation. Sections were taken in the sagittal plane with the dural side of the calvaria as the bottom of the image. Groups were analyzed using hematoxylin and eosin (H&E) to highlight new bone formation *versus* original colloidal material. Zoomed images correspond to the *boxed area* on the total defect area. *Scale bars* = 1 mm

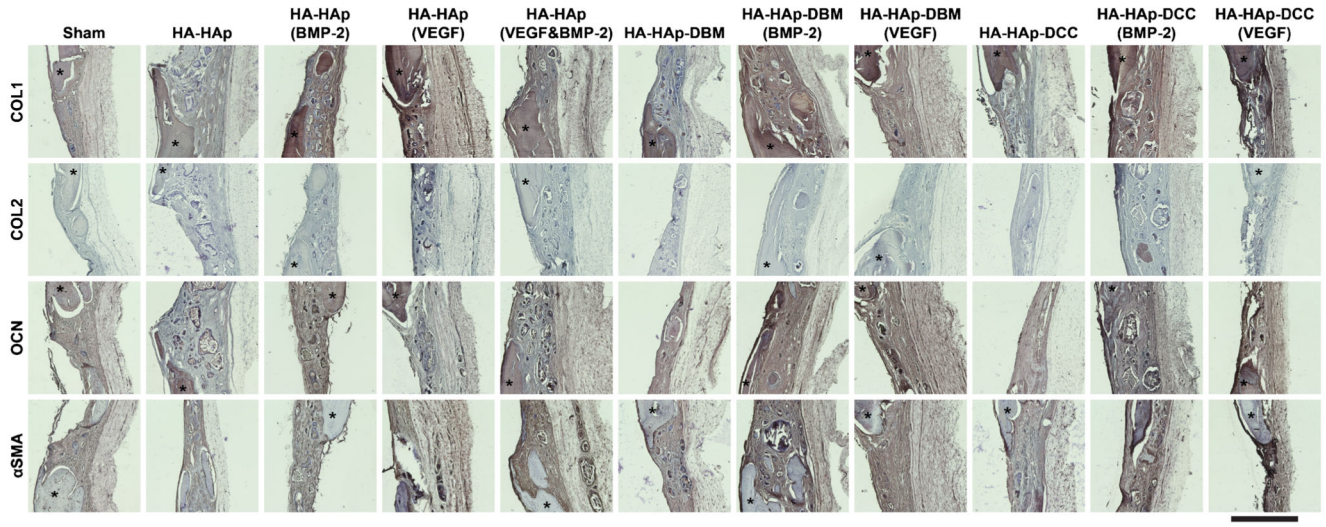

Fig. 5.

Immunohistochemistry (IHC) results for collagen 1 (*COL1*), collagen 2 (*COL2*), osteocalcin (OCN), and alpha-smooth muscle actin (*αSMA*). *Brown* coloring represents positive presence for the selected antibody, where *blue* staining represents negative antibody presence. All images represent *in vivo* healing of material groups after 8 weeks post-implantation. *Asterisk* corresponds to defect bone edge, *scale bar* = 1 mm